sciendo

DOI: 10.2478/awutp-2021-0005

ANNALS OF WEST UNIVERSITY OF TIMISOARA PHYSICS
Vol. LXIII, 2021

STRUCTURAL, CHEMICAL AND OPTICAL PROPERTIES OF PURE AND AL-DOPED ZnO THIN FILMS DERIVED BY SOL–GEL DIP COATING PROCESS

Ali sadek Kadari[a,e], Abdelkader Nebatti Ech-Chergui[b,e], Mohamed walid Mohamedi[b], Abdelhalim Zoukel[c], Tair Sabrina[b], Adjdir Mehdi[d], Kouider Driss-Khodja [a,e], Bouhalouane Amrani[a,e]

[a] *Electron Microscopy Center, Faculty of Exact and Applied Sciences, University of Oran1 Ahmed Ben Bella, Oran, Algeria*
[b] *Laboratory of Materials Sciences and Applications (LSMA), University of AinTemouchent Belhadj Bouchaib, faculty of sciences and technology, Algeria*
[c]*Platform of Physico-Chemical Analysis (PTAPC-Laghouat-CRAPC), Laghouat, Algeria*
[d]*Applied Organic Synthesis Laboratory, Faculty of Exact and Applied Sciences, University Oran1 Ahmed Ben Bella, BP 1524 El M'Naouer, 31000, Oran, Algeria*
[e]*Laboratory of Theory and Simulation of Materials, Faculty of Exact and Applied Sciences, University of Oran1 Ahmed Ben Bella, Oran, Algeria*
**Corresponding author: abdelkader.nebatti@daad-alumni.de*

Article Info

Received: 03.05.2021
Accepted: 14.06.2021

Keywords:
Sol–gel method; ZnO thin film; Aluminum doping; XRD; SEM; Optical properties.

Abstract

Pure and Al-doped ZnO thin films were successfully deposited with sol-gel dip coating on both substrates Si (100) and glass. The structural, chemical, morphological and optical properties as a function of the annealing temperature and dopant atomic concentration were investigated by means of X-ray diffraction, Energy dispersive X-ray, Scanning Electron Microscopy, and spectrophotometry. All the pure and doped films show a polycrystalline nature and hexagonal in structure. Accurate doping was proven by EDX. In addition, the SEM analysis revealed that the films possess uniform distribution throughout the surface and the grain dimension decreases with Al doping. From the transmittance measurements, it is see that all films are over 55% in the visible region and the band gap energy increases from 3.28 to 3.45 eV with the increase of Al concentration.

1. Introduction

ZnO is a II-VI semiconductor with a large and direct bad gap, high exciton binding energy, high transmittance in the visible region, high chemical and thermal stability, and non-toxic nature. Due of their excellent electrical and optical properties, ZnO has attracted big importance at recent years because of its potential uses in optoelectronic and transparent electronic devices [1, 2] . ZnO can be doped with a wide variety of ions to meet the demands of several application fields. Among the different dopants, Doping ZnO with group III elements such as boron [3] , gallium [4], and aluminium [5]. improves several properties such as resistivity and transmittance without compromising optical transmission. As a result, X-doped ZnO (X= B, Ga , Al) is being discussed as a transparent conducting oxide (TCO) with potential applications such as front electrodes in solar cell devices [6] or temperature sensors [7]. In addition to that, ZnO doping is achieved by atoms of higher valence elements such as In^{+3}, Mo^{+6}, Al^{+3} replacing Zn^{+2}. Aluminum is abundant, cheap, untoxic and can be an excellent applicant for dope ZnO among Group III as a whole. Many techniques were used for fabrications of ZnO thin films for example radio frequency magnetron sputtering[8], spray pyrolysis[9, 10], chemical vapor deposition [11],electrochemical deposition[12] and sol-gel processing[13, 14]. Among these techniques, sol-gel [7] has attracted great interest for obtaining thin films due of its great advantages: simplicity, reduced cost, wide area substrate coating and simple to realized doping incorporation. In this work, pure and Al-doped ZnO thin films were deposited on Si (100) substrates and glass substrates by the dip coating process, we show the effects of annealed, and Al doping on the structural, morphological and optical properties of the films were investigated.

2. Experimental details

Each sol was synthesized from a Zinc acetate Zn ($CH_3CO_2)_2$. 2 H_2O precursors were dissolved in 2-methoxyethanol and Monoethanolamine (MEA). The molar ratio of MEA to zinc acetate was maintained at 1.0, and the concentration of Zn ($CH_3CO_2)_2$. 2 H_2O was 0.75 mol/L, under vigorous stirring at 60 C for 30 Minuten, this solution of un-doped material.
The gel films were fabricated by dipping a silicon and glass substrate in the coating solution.
Al doping solution was prepared from Aluminum Chloride $AlCl_3$, the amount of Aluminum, defined by 100[Al]/ [Al+Zn] was varied over a range of 0-5.at. %. The structural aspect of the Sol-Gel films was investigated by X-ray diffraction (model Bruker D8 Advance) using Cu Ka radiation (λ = 1.5406 A °) and operating at 40 KV and 40 mA, the film attachment was used. 2 θ- scans from 30 to 70^0

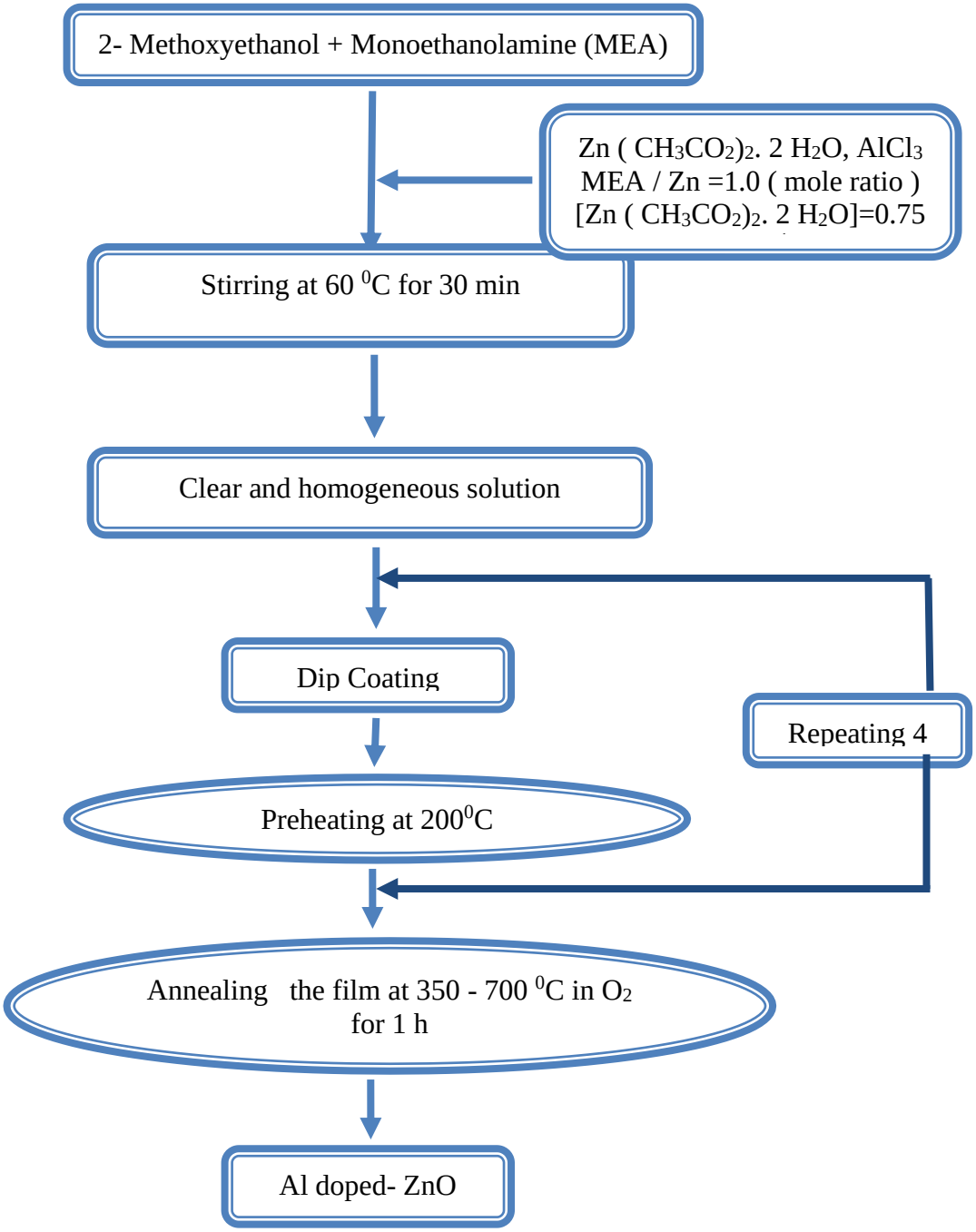

Figure 1. Flowchart showing the procedure for preparing the aluminum-doped ZnO.

3. Results and discussion

3.1. Silicon substrate

XRD shows pattern for ZnO films annealed from 300 ^{o}C to 700 ^{o}C in O_2 (Figure 2). For the films annealed at 300 ^{o}C, no diffraction peak is observed. This indicates that film remains amorphous at/ or blow this temperature. For the sample fired at 350 ^{o}C, started of ZnO film, for the sample annealed at 450 ^{o}C, several strong diffraction peaks at $2\theta=32^{o}$, 34^{0},36°, 47°,57°,63°,68°,69° are present in the XRD pattern, which are assigned to (100), (002), (101),

(102), (110), (103), (112) and (201) diffractions of hexagonal wurzite ZnO respectively, suggesting the starting of crystallization at this annealing temperature. For the sample annealed at 550 C, show the same XRD for powder ZnO standard, with a=3.24992 A^o, c=5.20658 A^o, D=5.675 g/cm3. Further the increasing annealing to 700 ^{o}C, there is not very big alteration in level peaks.

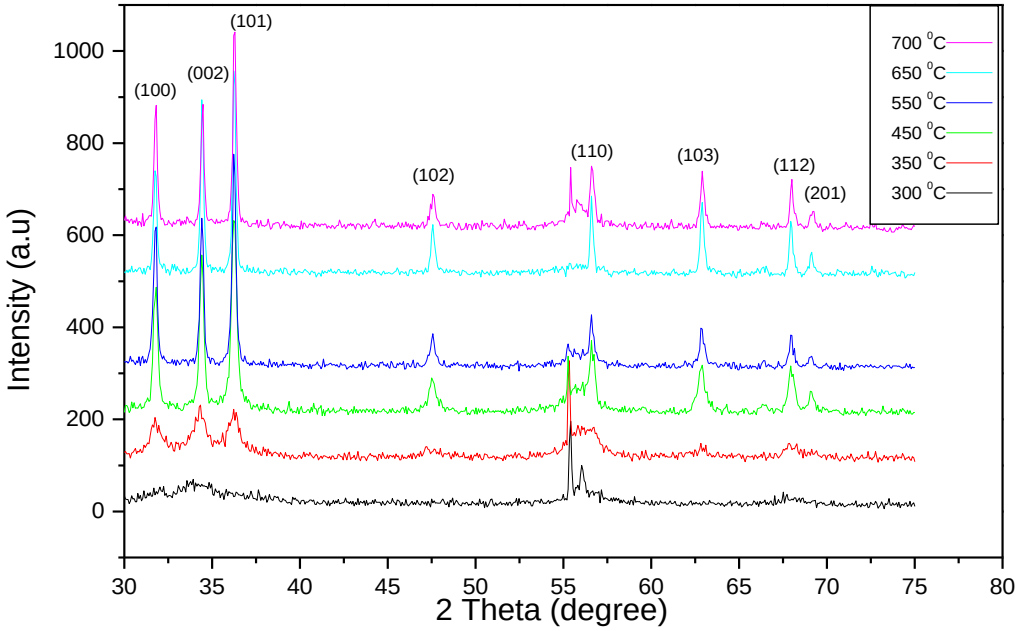

Figure 2. XRD patterns of ZnO films deposited on silicon substrate by Sol –Gel with Different annealing temperature in O_2

3.1.1 Effect of Aluminum content

Figure 3. shows XRD results of ZnO: Al with different Aluminum contents annealed at 550 ^{0}C in O_2, which were synthesized on Si substrates by sol gel method. It can be seen that the doping does not change the wurtzite structure of ZnO . The height of the ZnO peak relative to other reflection signifies the extent of c-axis orientation and hence film structural quality. Also we can note that the samples with ZnO: Al (3%) exhibit the preferential crystal orientation and important intensity of (002) peak. These result is well accord with the research results report by G.G. Valle et al[15]

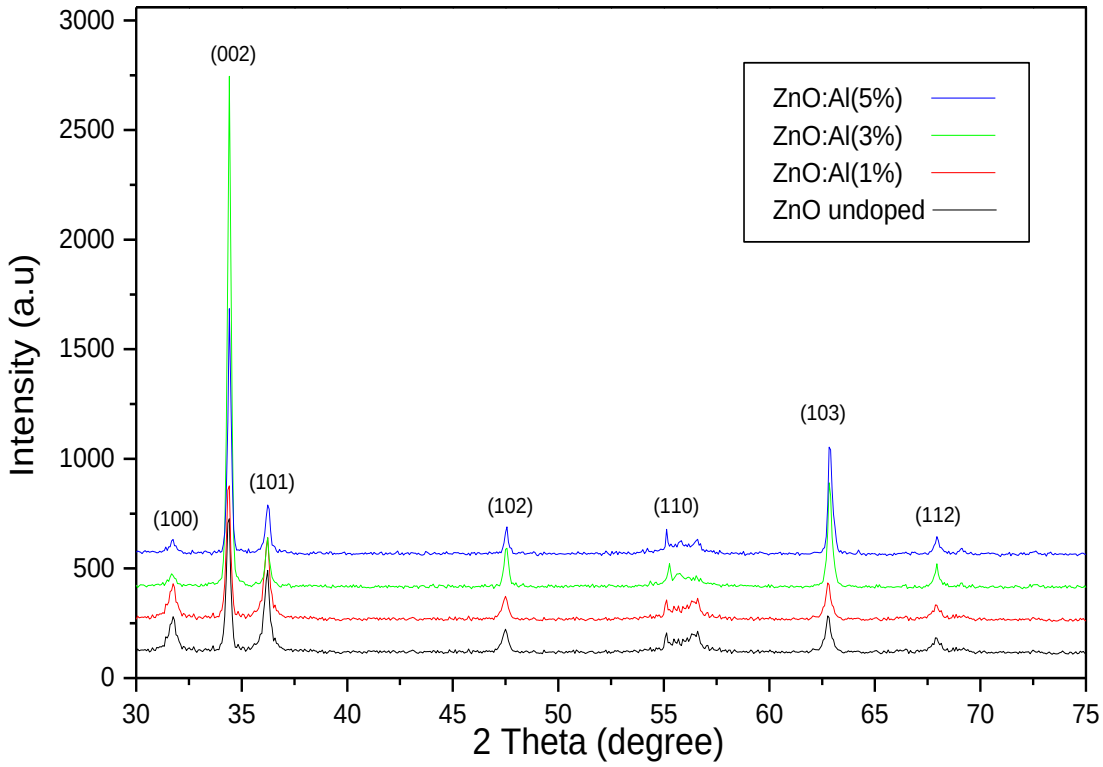

Figure 3. XRD patterns of ZnO:Al films deposited on silicon substrate by Sol –Gel with Different amount Aluminum annealed at 550 ^{0}C in O_2

It's worth noting that the texture coefficient TC(hkl) is calculated to offer an indication of the preferred orientation of the films along the diffraction plane , with the largest value (TC(hkl) > 1) indicating the preferred orientation in the specified (hkl) direction , which is associated with increase in the number of grains along that plane (hkl) [16].Table 1. summarizes the lattice parameters and the variation of texture coefficients TC (hkl) of (100), (002) and (101) plans with the amount aluminum. Note that the values of the texture coefficient of the (002) plane are higher than 1 and increases significantly from 1.299 to 2.531 in the Al-doped films indicating that the (002) peak are now preferentially oriented, On the other hand, the texture coefficient (101) planes decrease. Therefore, our results suggest that the addition of amount aluminum assists in promoting a preferred (002) orientation of the films. This result is similar to the research results reported by A. Mahroug and co-worker et al. [17]. In addition, as the relative intensity of the peak (002) was stronger than the other peaks, the films prefer c-axis orientation. This is due to relatively low surface energy (002) for planes [18].

Table 1. Lattice parameters and texture coefficient (100), (002) and (101) peaks of pure and Al-doped ZnO thin films.

Doping type	a [A°]	c [A°]	TC (100)	TC (002)	TC (101)
Undoped	3.24880	5.20540	0.940	1.299	0.763
ZnO:Al (1%)	3.24880	5.20540	0.212	2.496	0.293
ZnO:Al (3%)	3.25010	5.20710	0.585	2.504	0.271
ZnO:Al (5%)	3.25010	5.20710	0.176	2.531	0.215

$$TC(hkl) = \frac{I(hkl)/I_0(hkl)}{1/N.\sum nolimits_N [I(hkl)/I_0(hkl)]}$$

Where I (hkl) and I_0 (hkl) denotes the measured intensity and the intensity of the standard powder diffraction pattern, respectively, and N the number of considered reflections.

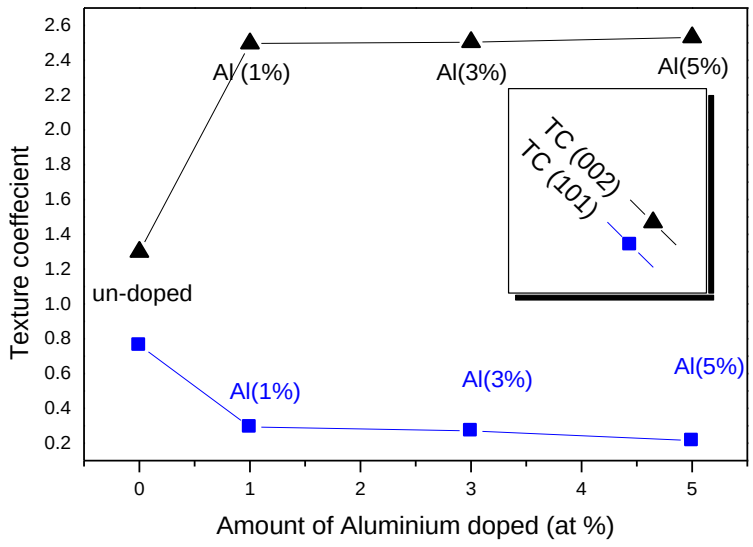

Figure 4. Variation of Texture coefficient of peak (002) and (101), pure and Al-doped with different amount Aluminum annealed at 550 ^{0}C

3.1.2 Effect of doping to the crystallite size

The crystallite size of the films, obtained from X-ray diffraction (XRD) at the Zinc oxide (ZnO) doped and pure (002), (101) plane, respectively, as a function of annealing temperature. I see that the crystallite size increased for both ZnO pure and doped, below 550 C, the shortage of crystallization energy caused low crystallinity in the film which resulted in

small crystallite size. Crystallite size D (hkl) of ZnO thin film was calculated with Scherrer's equation as [19]:

$$D_{(hkl)} = \frac{K\lambda}{\beta_{(hkl)} \cos\theta_{(hkl)}}$$

Where, 'D' is the crystalline size, 'K' is the constant (0.9), λ is the X-ray wavelength used, 'β' the angular line width of half maximum intensity and 'θ' is Bragg's diffraction angle

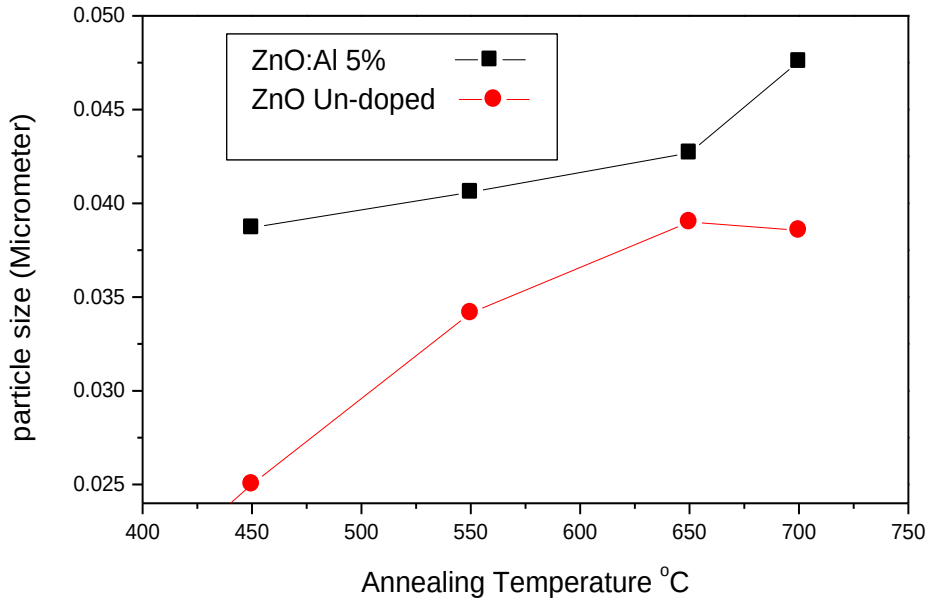

Figure 5. Variation of crystallite size of pure ZnO and ZnO:Al (5%) with different annealing temperature

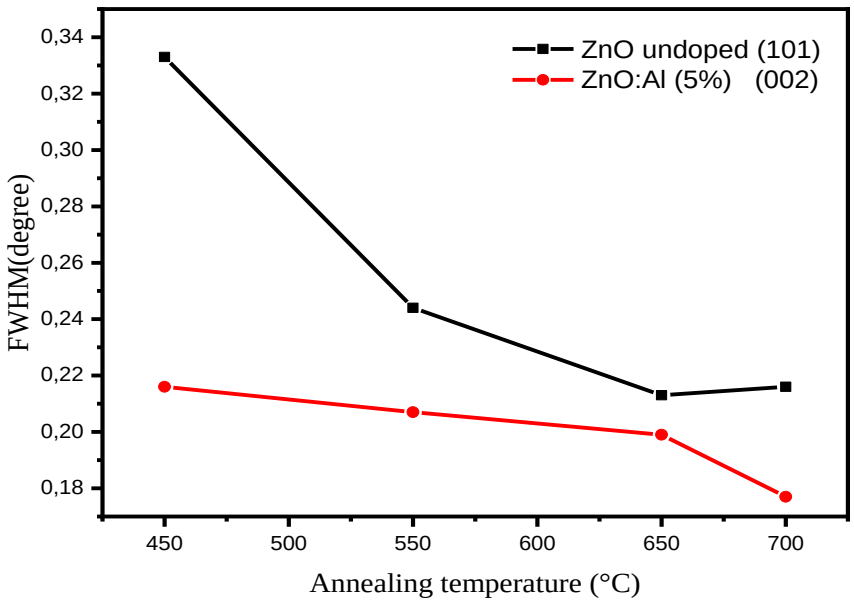

Figure 6. Variation of Full Width Half Maximum (FWHM) of pure ZnO peak (101) and ZnO:Al (5%) peak (002)with different annealing temperature

Figure 6 displays the full width at half maximum (FWHM) values of the films with the variation annealing temperature. The FWHM value decreases quasi linearly as the annealing temperature increases indicating a better crystallinity of the films with higher temperature. The decreased full-width at half-maximum (FWHM) was due to the decreased defect density induced by the lattice mismatch between the ZnO film and substrates

3.1.3 Annealing temperature and lattice parameter

The **c** and **a** parameters in Figure 7 were calculated using ZnO pure (101) peak position in Figure 2 and ZnO: Al (5 %) (002) peak position in Figure 3. There is no big different when you compare between **a** (doped and pure) and **c** (doped and pure), this mean that lattice parameters are independent of annealing temperature.

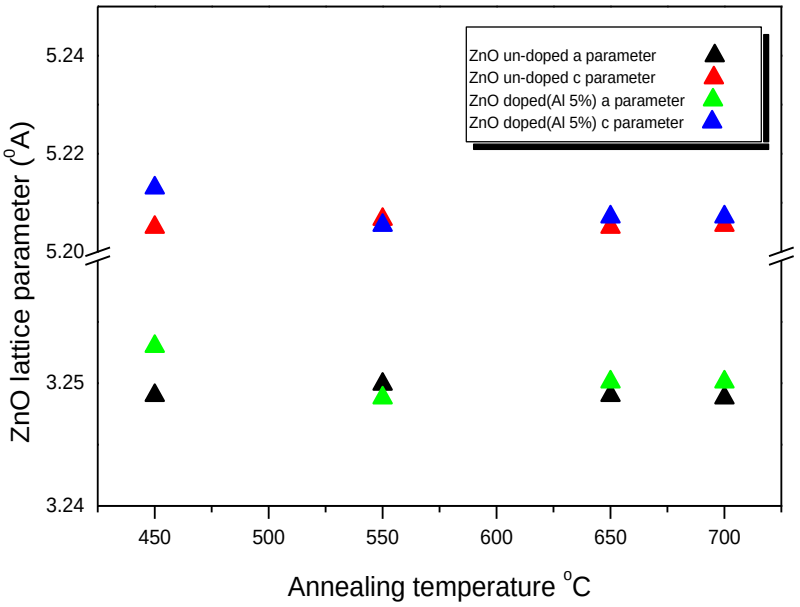

Figure 7**.** Variation of lattice parameters a and c on function annealing temperature

3.2 Glass substrate

We have also deposited ZnO films on Glass substrate and annealed at different temperature. The results are show in Figure 8. It is found that for the films annealed at 650 ^{o}C, no diffraction peak is observed, our film is damage in this temperature. The peaks are identified to (1 0 0), (0 0 2), (1 0 1), (1 0 2), (1 1 0), (1 0 3) and (1 1 2) plane of reflections for a single phase wurzite structure of ZnO. With annealing temperature increasing, the intensity of peak (101) peaks becomes stronger slightly. It indicates that the prefer orientation of the films is weakly dependent on the annealing temperature.

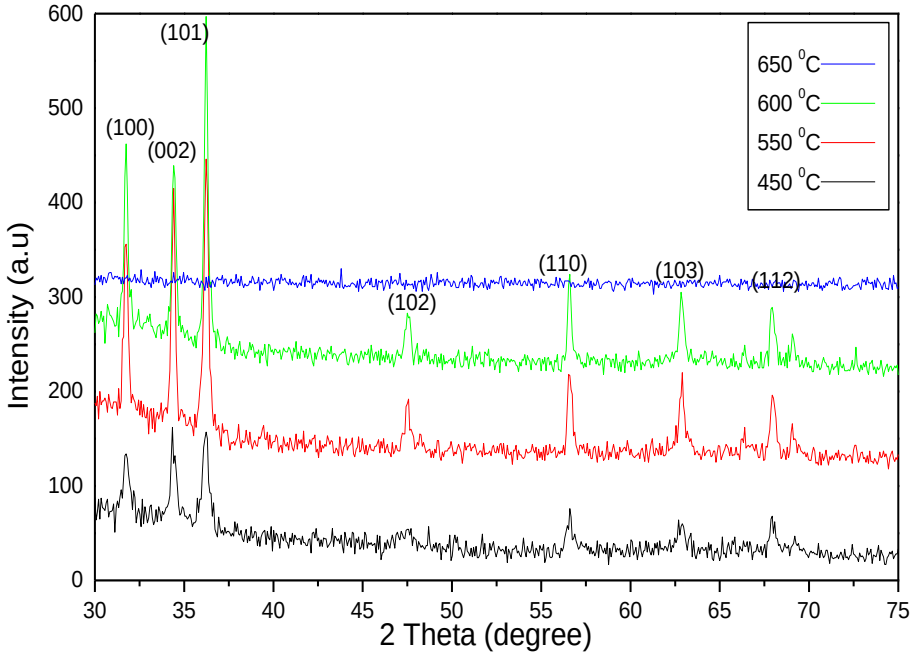

Figure 8. XRD patterns of ZnO films deposited on Glass substrate by Sol –Gel with Different annealing temperature in O_2

3.2.1. Effect of annealing temperature on the particle size

Figure 9 displays the variation of particle size of ZnO films peaks (101) with annealing temperature. It is found that the particle size increases almost linearly with increase annealing temperature. This is due to the improvement in the crystallinity of the films. So higher annealing temperature could promote the c-axis oriented growth and the crystallization of the Al doped ZnO thin films. Our findings are in line with those of earlier studies [20].

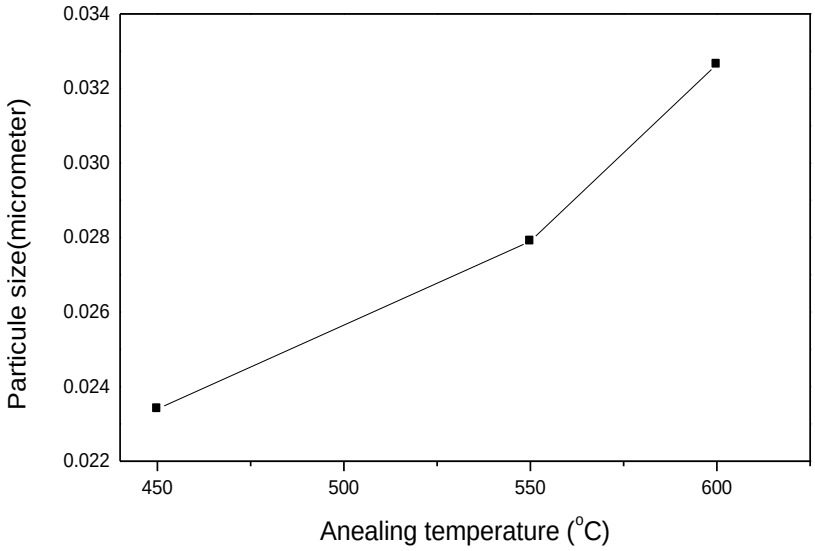

Figure 9. Variation of particle size of ZnO films peaks (101) with annealing temperature.

3.2.2. Effect of coatings to the thickness of the ZnO

The effect of the number of coating on the thickness of the ZnO films, Figure 10**,** was investigated by coating on glass substrate in the annealing temperature 450 ^{0}C in $O_{2.}$ As can be seen, that the thickness increases almost linearly with increase in the number of coating, which is behavior of typical characteristic of the technique of sol-gel spin coating technique. This could explain why crystallinity increases with film thickness. In ZnO films synthesized by sol-gel, Vinod Kumar et al. have observed similar behavior [21]

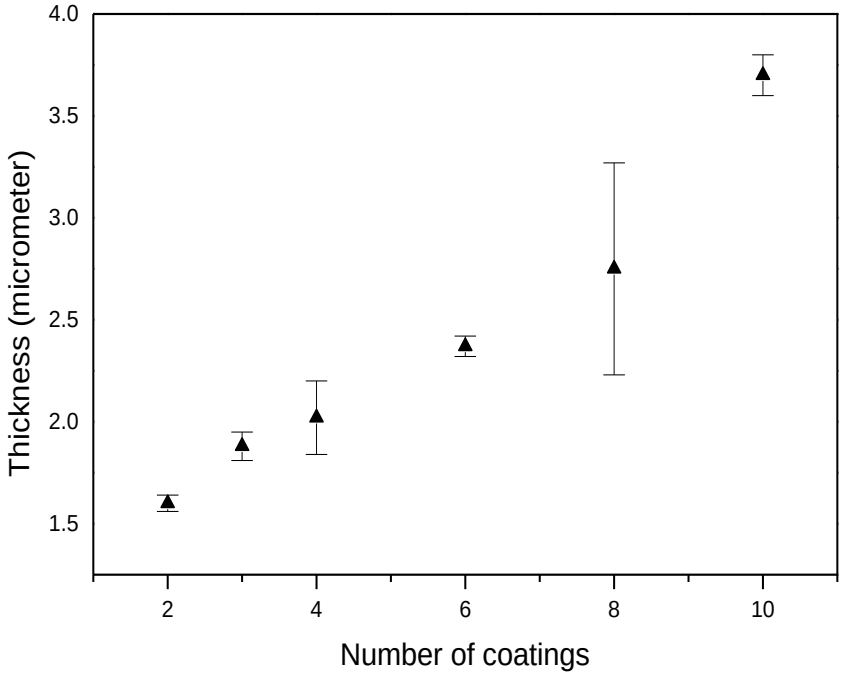

Figure 10. Thickness of ZnO flim with different times of coatings. All of the simples were annealed at 450 C in O_2

3.3 Morphological properties

The effect of Al doping on the surface morphology of ZnO thin films have been investigated using Scanning Electron Microscopy (SEM). Figure 11 shows the surface morphology images of pure and Al-doped ZnO thin films. The SEM micrographs showed that the films have compact grain morphology, dense and no cracks are observed on wide scan area for all films. The surface morphology is considerably influenced by the quantity of aluminum incorporated in the ZnO films.

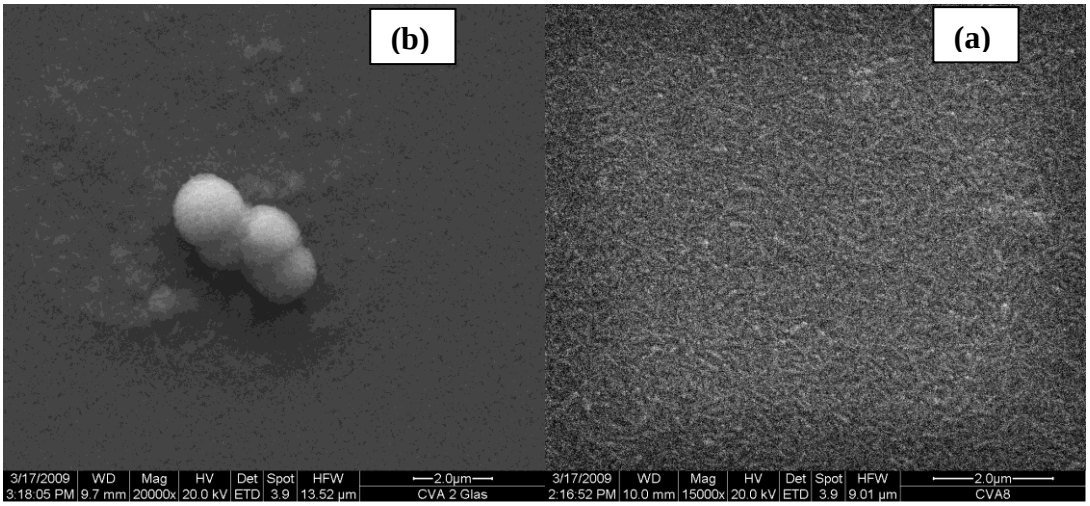

Figure 11. SEM images (top views) : (a) pure and (b) Al doped (5 %)

3.4. Chemical composition

The chemical compositions of the obtained films by dip coating approach were analysed via energy dispersive x-ray (EDX) (Figure 12 a and b). Figure12 (a) shows the typical EDX spectra of one pure and one Al (1%)-doped ZnO film. They clearly show the presence of zinc, oxygen, and (the upper spectrum only) aluminium clearly confirming the doping of the film. As regards, the Figure 12(b) shows the Al/Zn-concentration within the films as function of the Al/Zn concentration introduce in the solution. Figure 12(b) clearly shows that the aluminium concentration within the films increases linearly with the Al/Zn concentration introduced into the solution. It should mention that each data point is the average of three EDX measurements. Further, the error is the standard deviation.

3.5. Optical properties

The optical transmittance spectra of thin films in the wave- length ranging 300-800nm in room temperature are represented in Figure 13**.** All films have average transmittance over 50% in the visible area. The band gap (Eg) was estimated using a $(\alpha h\nu)=C(h\nu-Eg)^{1/2}$ relationship, where α is the absorption coefficient, C is a constant and hν is the photo energy.

The absorption coefficient α of the films has been calculated by using the equation $\alpha=(1/d)\ln T$, where T is the transmittance and d is the film thickness. The band gap was determined with extrapolation of the linear area of $(\alpha h\nu)^2$ against the photo energy. As shown in the inset in Figure 14 the optical band gap energy increased from 3.28 to 3.45eV by increasing Al concentration; the increased in the band gap may be due to the Burstein-Moss effect [22] .

These values band gap are in a good agreement with the reported work by Jin-Hong Lee and co-workes (3.28 to 3.30 eV) by doping more than 3 at.% [23].

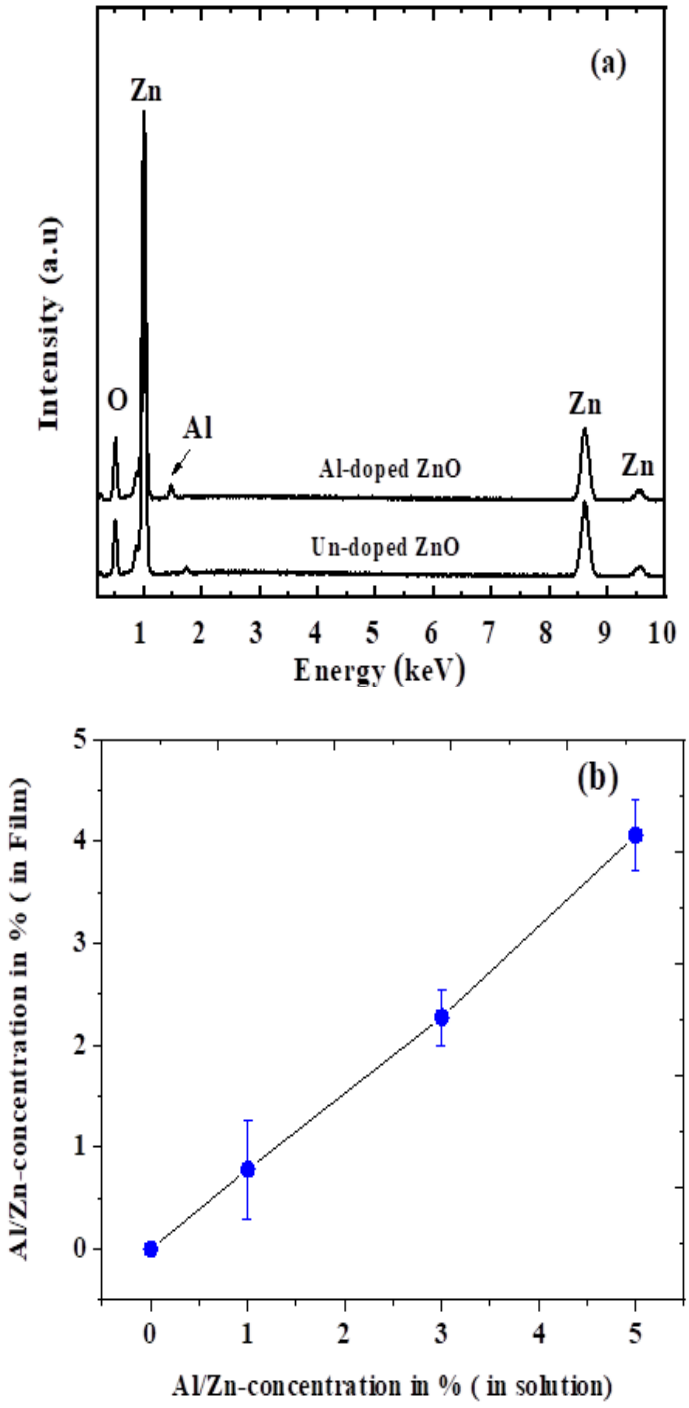

Figure 12. EDX-analysis of the synthesis films: (a) shows the typical EDX spectra of one un- doped and one Al-doped ZnO-film. (b) shows the Al/Zn- concentration within the films as function of the Al/Zn- concentration

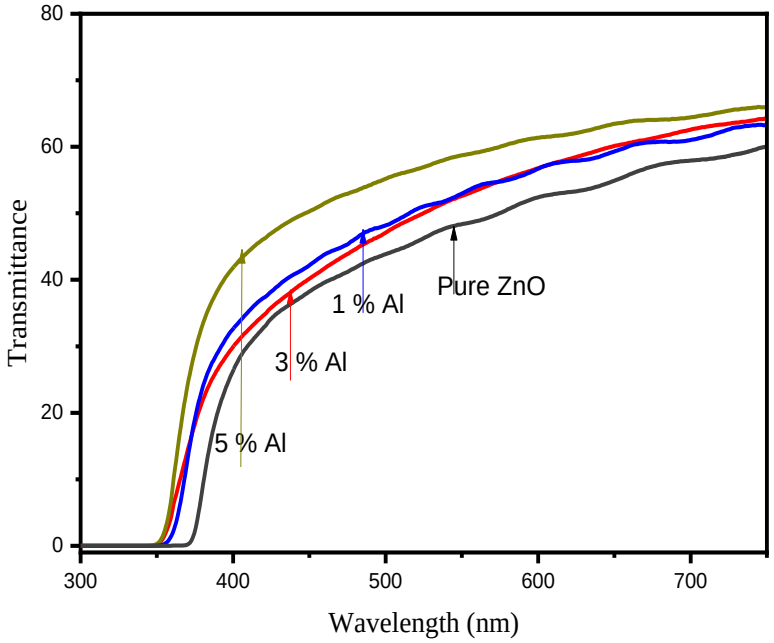

Figure 13. Optical transmittance spectra of pure and Al doped ZnO films on borosilicate glass for different dopant concentration

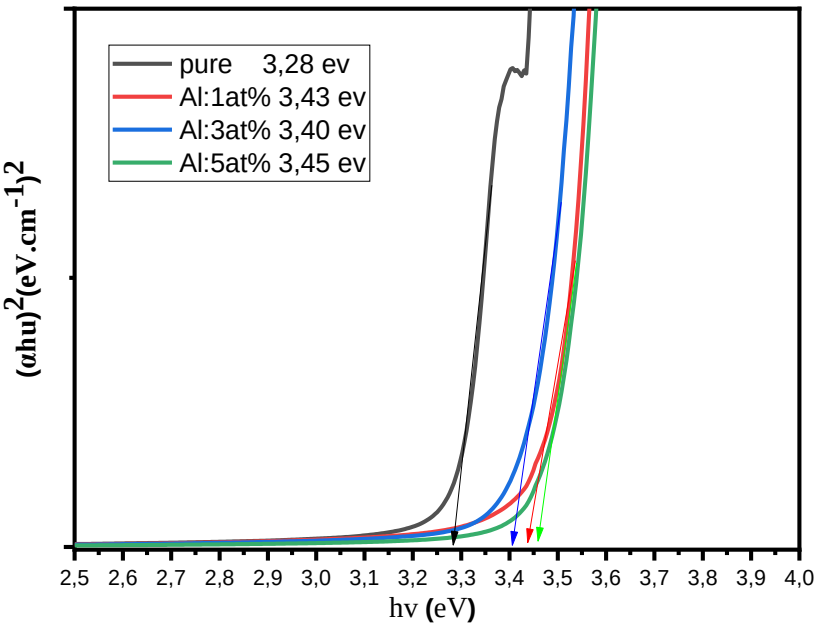

Figure 14. Optical band gaps of pure and Al doped ZnO films on borosilicate glass for different dopant concentration

To compare our band gap data of the Al-doped ZnO films with values from literature. For films by spin coating, A. Mahroug et al. found that the optical band gap energy increases with increasing Al concentration [17]. Moreover, S. Venkatachalam et al [24], observed analogous behaviour. Our results are consistent with the results of previous studies.

4. Conclusion

Pure and Al-doped ZnO thin films were successfully deposited on Si (100) substrates and glass substrate by the cost effective sol–gel dip coating method. The influences of annealing treatment and Al doping on structural, morphological and optical properties of pure and Al-doped ZnO thin films were investigated. The XRD spectra confirmed that the films were of hexagonal in structure. The grain size of crystallites increases with increasing in Al concentrations. SEM images revealed the formation of granular surface. The doping with Al, can be easily controlled by varying the concentration of Al in the solution. Precise Al doping was possible as proved by EDX. The transmittance measurements of all films is over 55% in the visible range and the band gap energy increases from 3.28 to 3.45 eV with increase of Al concentration, showing that Al doping has an influence on the energy band structure of ZnO.

References

[1] S. Liang, H. Sheng, Y. Liu, Z. Huo, Y. Lu, H. Shen, Journal of crystal Growth, 225 (2001) 110-113.

[2] W. Yen, Y.-C. Lin, J. Ke, Applied Surface Science, 257 (2010) 960-968.

[3] Z.N. Kayani, Z. Bashir, S. Riaz, S. Naseem, Z. Saddiqe, Journal of Materials Science: Materials in Electronics, 31 (2020) 11911-11926.

[4] G.D. Yuan, W.J. Zhang, J.S. Jie, X. Fan, J.X. Tang, I. Shafiq, Z.Z. Ye, C.S. Lee, S.T. Lee, Advanced Materials, 20 (2008) 168-173.

[5] T. Kim, D. Choo, Y. No, W. Choi, E. Choi, Applied Surface Science, 253 (2006) 1917-1920.

[6] S. Neubert, M. Wimmer, F. Ruske, S. Calnan, O. Gabriel, B. Stannowski, R. Schlatmann, B. Rech, Progress in Photovoltaics: Research and Applications, 22 (2014) 1285-1291.

[7] A. Nebatti, C. Pflitsch, B. Atakan, Thin Solid Films, 636 (2017) 532-536.

[8] W. Yang, Z. Liu, D.-L. Peng, F. Zhang, H. Huang, Y. Xie, Z. Wu, Applied Surface Science, 255 (2009) 5669-5673.

[9] B. Ergin, E. Ketenci, F. Atay, International journal of hydrogen energy, 34 (2009) 5249-5254.

[10] N. Tarwal, P. Patil, Applied Surface Science, 256 (2010) 7451-7456.

[11] C. Pflitsch, A. Nebatti, G. Brors, B. Atakan, Journal of crystal growth, 348 (2012) 5-9.

[12] Z. Yin, S. Wu, X. Zhou, X. Huang, Q. Zhang, F. Boey, H. Zhang, small, 6 (2010) 307-312.

[13] V. Musat, B. Teixeira, E. Fortunato, R. Monteiro, P. Vilarinho, Surface and Coatings Technology, 180 (2004) 659-662.

[14] J.-H. Lee, B.-O. Park, Thin solid films, 426 (2003) 94-99.

[15] G. Valle, P. Hammer, S.H. Pulcinelli, C.V. Santilli, Journal of the European Ceramic Society, 24 (2004) 1009-1013.

[16] B. Joseph, P. Manoj, V. Vaidyan, Ceramics International, 32 (2006) 487-493.

[17] A. Mahroug, S. Boudjadar, S. Hamrit, L. Guerbous, Materials Letters, 134 (2014) 248-251.

[18] U. Yogeswaran, S.-M. Chen, Sensors, 8 (2008) 290-313.

[19] B. Cullity, Readings, MA, (1978) 102.

[20] J. Li, J. Xu, Q. Xu, G. Fang, Journal of alloys and compounds, 542 (2012) 151-156.

[21] V. Kumar, N. Singh, R. Mehra, A. Kapoor, L. Purohit, H. Swart, Thin solid films, 539 (2013) 161-165.

[22] F. Shan, Y. Yu, Journal of the European Ceramic Society, 24 (2004) 1869-1872.

[23] J.-H. Lee, B.-O. Park, Materials Science and Engineering: B, 106 (2004) 242-245.

[24] S. Venkatachalam, Y. Iida, Y. Kanno, Superlattices and Microstructures, 44 (2008) 127-135.